

3D Electrical Resistivity Tomography of Karstified Formations Using Cross-Line Measurements

Maurits Van Horde¹, Thomas Hermans², Gael Dumont³,
and Frédéric Nguyen⁴(✉)

¹ Dredging International NV, DEME-Group, Zwijndrecht, Belgium

² Stanford University, Stanford, USA

³ University of Liège, Liège, Belgium

⁴ KU Leuven, Leuven, Belgium

f.nguyen@ulg.ac.be

Abstract. Limestone formations constitute a serious geological challenge for large building projects such as wind turbine farms. Indeed, limestone formations might be subject to karstic phenomena such as sinkholes or subsidence constituting a serious hazard for existing constructions and future civil engineering projects. In calcareous geological settings, a characterization of the subsurface to detect wealthy rocks is therefore mandatory. The classical approach consists in drilling boreholes and cone penetration tests to identify subsurface properties. However, they only provide punctual information whereas karstic environments show sharp variations with complex 3D geometry, making interpolation between boreholes relatively inefficient. In this context geophysical methods can provide spatially distributed information at a limited cost. In particular, surface electrical resistivity tomography (ERT) aims at mapping the distribution of electrical resistivity in the subsurface in a passive way using only surface sensors. The method is based on the measurement of electrical potential resulting from the injection of DC electrical current. In karstic contexts, weathered rocks generally show an increased porosity and water content compared to healthy limestones, leading to strong contrasts in their electrical resistivity. ERT is therefore particularly sound to investigate karstic phenomena. Most standard ERT applications use 2D profiles that are quick to acquire and interpret. However, in complex 3D geometries, the acquisition of 2D profiles is not sufficient to image correctly subsurface structures. 3D data sets require more efforts both for acquisition and interpretation, making their use more costly and therefore less common in practice. In this contribution, we propose an innovative 3D ERT acquisition procedure to reduce the field efforts and duration of the 3D acquisition procedure. The method is based on standard 2D parallel lines, but, in contrast with previous methodologies, we also acquire cross-line measurements in several directions to increase the ability of ERT to image 3D structures. To ensure a fast acquisition of large area, we limit the cross-line measurements to pre-defined line spacing and implement a roll-along technique moving previously acquired 2D lines in the perpendicular direction. The data can then be acquired with a standard 64 electrodes equipment. We first demonstrate the increased imaging capacities of our technique compared to standard acquisition methods with a numerical benchmark. Then, we validate it through a field application to detect the 3D geometry

of karstic features and unaltered limestone formations. We analyze the minimum amount of cross-line measurements required for a proper imaging of the 3D structures. The proposed 3D survey induces extra costs of about 50% compared to a traditional 2D survey, but this extra cost is compensated by a largely better imaging of the subsurface. This cost will be reduced in the future by optimization of the survey to reduce acquisition time.

Keywords: 3D electrical resistivity tomography · Karstic environments · Cross-line measurements · Electrode configuration

1 Introduction

In the last two decades, electrical resistivity tomography (ERT) has been widely applied in many different contexts. The wide range of applications of ERT is a result of the large number of parameters influencing the electrical resistivity of the subsurface (porosity, fractures, rock/soil type, saturation, temperature, fluid electrical conductivity, etc.) and the robustness of the method. However, the standard use of ERT remains the collection of 2D subsurface profiles. Because of the simplicity of field implementation, requiring only one to two people for a couple of hours, 2D surveys are not time-consuming and relatively cost-effective. In addition, acquisition times have drastically decreased with the advent of multi-channel systems and automated switching systems [1]. Nevertheless, one of the major drawbacks of 2D survey is the underlying assumption that the subsurface is actually 2.5D, i.e. that electrical resistivity is constant in the direction perpendicular to the profile. This assumption enables to successfully reduce the complexity of forward modeling from 3D to 2D using a Fourier-cosine transformation [2]. Most interpretation software, commercial or academic, uses this assumption in the inversion of 2D data sets. This assumption can be valid for certain conditions (profile perpendicular to main geological structures, relatively homogeneous subsurface), but it can also lead to distorted and misleading results in strongly variable and heterogeneous environments [3], such as encountered in karstic settings. In such cases, or when a detailed mapping of the subsurface is required, 3D acquisition and inversion techniques must be considered. This is particularly true for karstic hazard, an engineering target suited for ERT given its sensitivity to electrical resistivity, where the 3D nature of the dissolution processes makes the 2.5D hypothesis of the subsurface much weaker than for fault imaging for example.

In this paper, we propose an innovative 3D acquisition procedure based on the roll-along technique of [4]. It makes use of 2D parallel lines with additional cross-line measurements. However, in order to increase the number of directions represented in the data, we propose to use cross-line measurements in several directions as proposed in [5] for imaging seepage in an embankment. Those cross-line measurements are based on dipole-dipole configurations as commonly used in cross-borehole surveys. We illustrate the method by investigating the subsurface geometry in a karstic environment for a future wind turbine project. We first describe the field site and the geological context. Then, the designed acquisition and processing procedure is described and assessed by numerical benchmark modeling, using a synthetic model. We applied our validated methodology to the field case to image the top of the

unaltered limestone formation and to characterize the 3D geometry of karst features. We then discuss the importance of cross-line measuring and analyze its capability and optimal setup for correct subsurface geometry imaging.

2 Site Description

The test site is located in the Couvin region, Belgium (Fig. 1). It is a large unbuilt area where a wind turbine construction project is ongoing. The survey site region is located at the southwestern edge of the synclinorium of Dinant. This geological structure composed of a succession of sedimentary rocks was folded during the Variscan orogeny. The succession of sedimentary formations is the result of the Devonian transgression towards the north which is actually made up of a succession of transgressive and regressive phases. This enables to observe the progression of terrigenous clastic sedimentation of the lower Devonian to carbonated sedimentation, which characterizes the Middle Devonian, to the Upper Devonian base including the establishment of reef systems built up by biostromes of the Eifelian (Couvinian) and bioherms of the Givetian [6]. These periods of carbonate production are interrupted by episodes of terrigenous sedimentation of various sizes. In the region of the survey site, limestone can be locally highly fractured and karstified. Karst features are generally filled with clayey sandstones of the Cenozoic and sediments of the Oligocene [7].

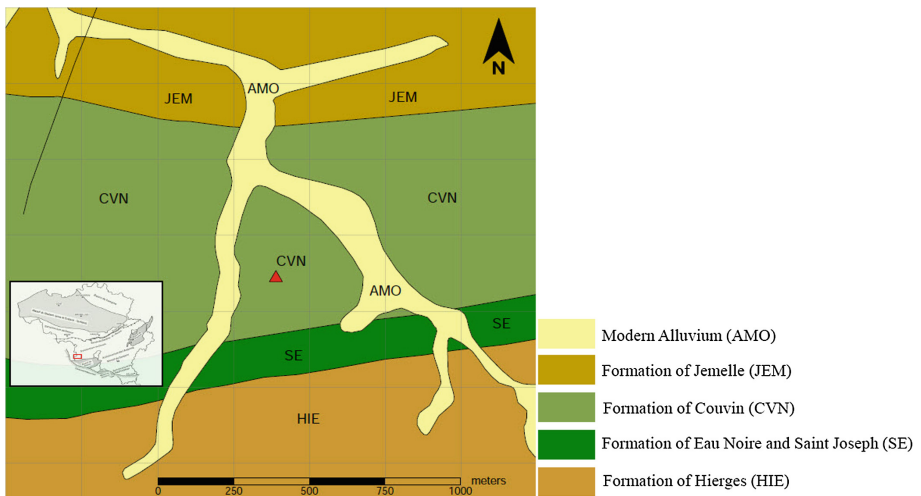


Fig. 1. Geological map of the site location. Red triangle represents the study area (modified after [6]).

In the study area, there are three major lithostratigraphic units (Fig. 1). The oldest is composed of the formations of Saint-Joseph and Eau Noire, which are lower Devonian in age. It consists of layers of shale and thin limestone. The second oldest formation is the formation of Couvin, from the middle Devonian. It consists of very thick and compact succession of limestone layers. It was formerly used for production

of lime and stone used in the construction industry as well as for iron ore exploitation contained within karstic features filled with sediment. The youngest formation is the formation of Jemelle, also from the Middle Devonian. It mostly consists of shale layers.

Shallow karsts constitute a serious hazard to existing constructions and for civil engineering projects of all scales [8]. Constructions on top of paleokarst features may not be safe due to the risk of resurgence, subsurface sinkhole development and subsidence which can cause serious damage to infrastructures [9]. A karstic system can become unstable and severely compromise structural integrity and stability of the whole construction. This is why the subsurface geometry needs to be very well characterized in a systematic way when constructing in limestone settings [10]. In the study area, paleokarstic phenomena are present and may be reactivated due to the present hydrogeological setting.

3 Electrical Resistivity Tomography

3.1 Survey Design

The main objective of our survey design was to use the ABEM Terrameter LS (64 electrodes) equipment which is routinely used to execute 2D-ERT surveys. It was decided to use a set of 18 parallel profile lines of 32 electrodes in combination with cross-line electrical resistivity measuring (Fig. 2), applying the 3D roll along technique

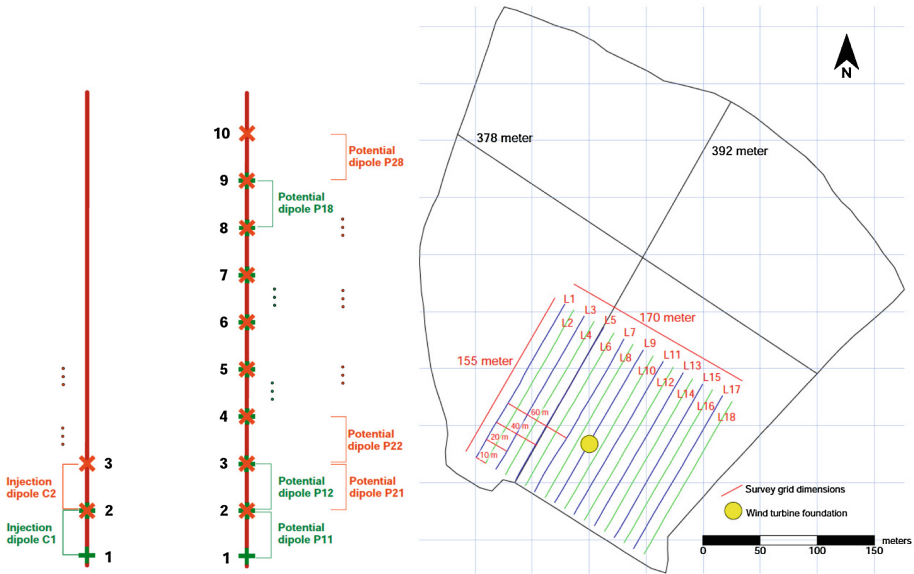


Fig. 2. Left: Cross-line measurement concept. Red lines indicate the electrode cables (2 per profile line). Electrode location for two different injection dipole are indicated with green and orange crosses respectively. Right: Survey site geometry is depicted by a dark grey line. Blue lines indicate lines of survey 1, green lines indicate lines of survey 2. Together they form the combined survey lay-out. The profile line ID number is indicated in red. The yellow dot is the location of the future wind turbine.

to progress laterally through the designed survey grid, connecting only 64 electrodes at a time. In-line measurements were performed along each line, and cross-line measurements were performed in between parallel profile lines with a certain offset with respect to a fixed chosen profile (Fig. 2 and Table 1). The latter contain 3D resistivity information on the subsoil in between parallel lines. The in-line electrode spacing is 5 m whereas the cross-line electrode spacing is 10 m. Since there are 18 profile lines in total, the combined survey grid consists of 576 electrodes. All electrodes were precisely positioned using a Trimble G8 GPS system. An in-line electrode spacing of 5 m was used to reach a sufficient depth of penetration for this site specific scenario since the pile foundations of the wind turbine will penetrate the surface up to 20 meters deep. Given the protocols used, this corresponds to a total number of 34644 measurements.

Table 1. Different dataset combinations made for three dimensional inversion with RES3Dinv®. ALL IL means all in line, ALL CL all cross-lines, CL # means that only the cross-line with # spacing has been used

	Combination of datasets	Number of datapoints in protocol	Number of datapoints after processing
Survey 1			
All IL + All CL	9 in-lines + 21 cross-lines	17322	12239
Survey 1 + Survey 2			
All IL	18 in-lines	7848	6721
All IL + CL 40	18 in-lines + 14 cross-lines	16780	12925
All IL + CL 60	18 in-lines + 12 cross-lines	15504	12264
All IL + All CL	18 in-lines + 42 cross-lines	34644	25469

3.2 Inversion Parameters

All the inversions were carried out with the same inversion parameters in the software RES2DINV®. We use a L1 norm on the data to reduce the effect of possible outliers and a L1 norm on the model [11] to favor sharp contrasts of resistivity as expected in karstic formations. The inversion process made use of an incomplete Gauss-Newton scheme.

Despite, the low variance of the measured apparent resistivity, the final error of the inversion of the full data set was still relatively high (more than 13%). In consequence, the data set was further trimmed post-inversion based on the individual misfit of each simulated measurement versus the observed one. We removed data points with a misfit greater than 20% (5300 data). This reduced the RMS data misfit to about 6% for the full data sets (all in-line and all cross-line). For a fair comparison, other subsets were built based on this sorted/trimmed full data set. We stopped the inversions when the RMS data misfit reached a value between 5 and 6%.

3.3 Results for the Synthetic Benchmark

To validate if our designed survey method can solve and image an artificially pre-defined 3D geological structure, a numerical benchmark model is carried out and field resistivity measurements are numerically simulated. If the synthetic 3D resistivity model based on these numerically simulated resistivity data corresponds well to the initial defined geological structures, we can conclude that the designed survey methodology is capable of solving similar 3D-subsurface geometries. For synthetic modelling, a karstic environment was chosen similar to the environment expected at the site under investigation. The numerical geological structure consists of a central ridge of competent limestone bedrock with karstic features on the sides. The different geological units present are the sediment cover, 10 m thick (55 Ω .m), weathered limestone with debris (450 Ω .m), ghost rock and tertiary sandstone filling karstic features (250-300 Ω .m) and unaltered limestone bedrock (750-2500 Ω .m). RES3DMOD® is used to numerically simulate the apparent resistivity data corresponding to a pole-pole survey. The most important structure within the context of wind turbine project is to detect the position of the unaltered bedrock. We therefore use the detection of the shape and location of the central limestone ridge as an indicator of the performance of the survey. In the following figures, this characteristic of the model will be highlighted by the 600 Ω .m iso-surface.

The full data set contains all measurements, i.e. in-line and cross-line 20, 40 and 60 m for both surveys. It is expected that this brings the most valuable information on the 3D structure of the model. As it appears in Fig. 3, this data set enables to retrieve relatively accurately the location, depth and shape of the ridge in the middle of the model. This confirms the survey (in-line and cross-line spacing, number of parallel lines) was correctly designed. All the reduced data sets retrieve less accurately the ridge structure. First, it appears that the use of a unique survey, i.e. an inter-line spacing of 20 m, is not able to image correctly the subsurface. The only feature that is adequately detected is the low resistive zone located at the origin of the grid. The reduction of acquisition time must not be done in detriment of the resolution of the survey. This is confirmed by the use of the in-line data from both surveys which already gives a better overview of the 3D structure. The reason of this relatively good performance lies in the orientation of 2D lines perpendicular to the geological structures. However, the width and depth of the ridge are not as accurate as with the full data set.

Adding cross-line measurements to 2D lines clearly improves the results. In this case, given the depth of the structure, cross-lines 40 m and 60 m are the most informative. They enable to refine imaging of the 3D structure. In this specific case, this is clearly the cross-line 40 that approaches the true model with most accuracy.

3.4 Results for the Field Data

In the inversion of the full data set (Fig. 4), a subsurface structure is recognizable with a central ridge of unaltered limestone bedrock at a depth between 225 m TAW and 195 m TAW. On its sides, two karstic features are clearly visible. The first is a large zone of low resistivity value between $X = 0$ and $X = 50$ m, the healthy bedrock being detected at a depth of 195 m TAW only. The second is a smallest low resistivity zone located between $Y = 50$ m and $Y = 100$ m and $X = 75$ m and $X = 150$ m.

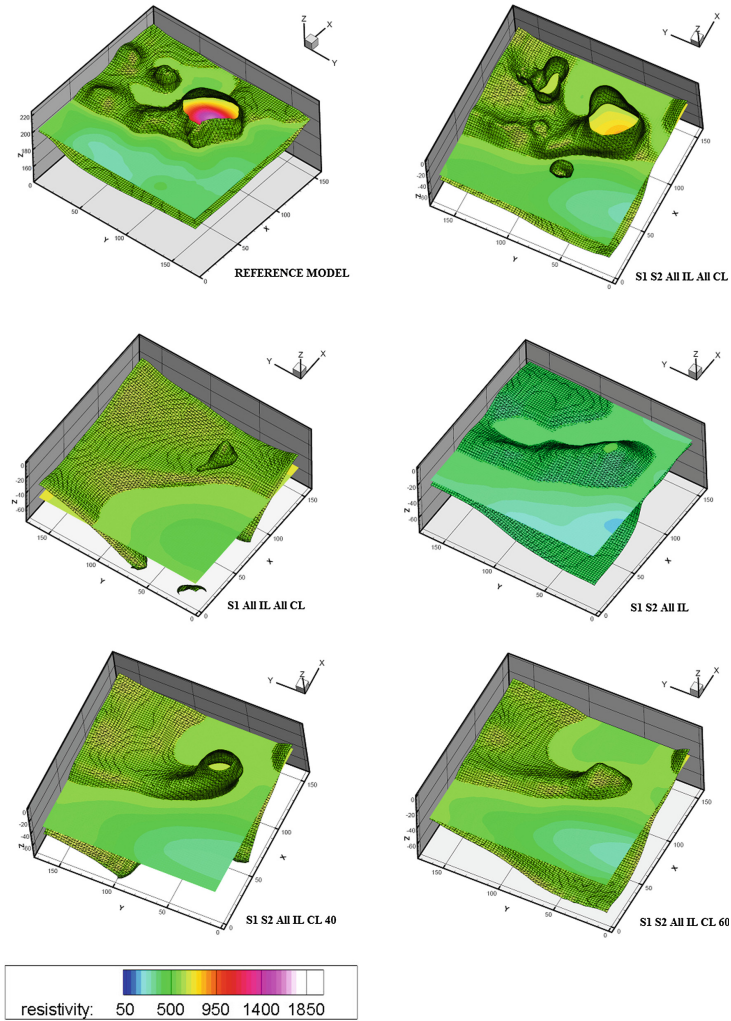


Fig. 3. Synthetic data inversion overview. Three dimensional block models of the subsurface resistivity distribution. The models show a resistivity iso-surface of 600 Ω .m representing the transition to altered limestone. The model annotation corresponds to the dataset combination overview provided in Table 1.

The inversion of reduced data sets confirms the observation made for the synthetic case. Clearly, the use of a spacing of 20 m between parallel lines is not sufficient to resolve the shape and location of the limestone ridge. This subset of data incorrectly locates the ridge as well as the second anomaly. The use of in-line data is sufficient to qualitatively detect most features of the subsurface geometry, but it is not accurate enough given the aim of the study. The depth of the unaltered bedrock seems to be found deeper down and the ridge does not appear as continuous. Also, due to a reduced

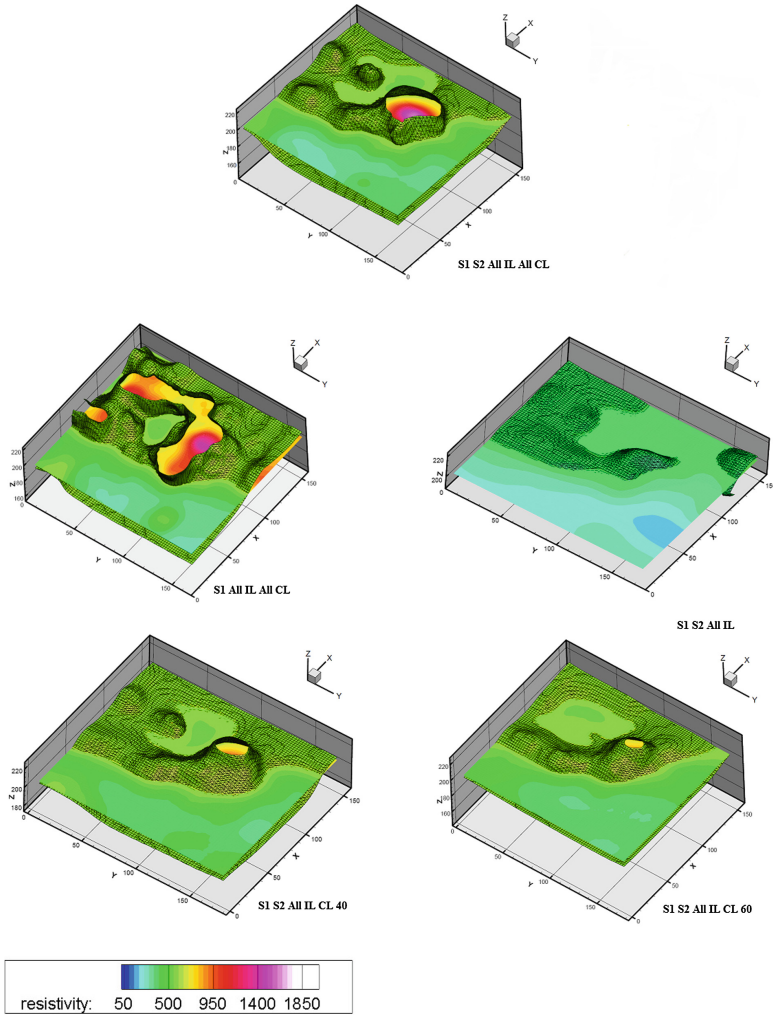


Fig. 4. Field data inversion overview: Three dimensional block models of the subsurface resistivity distribution. The models show a resistivity iso-surface of 600 Ω.m representing the transition to altered limestone. The model annotation corresponds to the dataset combination overview provided in Table 1.

depth of investigation and smaller coverage of the subsurface compared to cross-line data, this inversion images the first karstic anomaly as very low resistivity zone and is not able to detect the presence of healthy bedrock at depth.

Both inversions with additional cross-lines dipole (40 m and 60 m) manage to image the subsurface geometry as the full data set does. The data set with cross-line 40 m data seems to yield results the most similar to the reference, especially the second low resistivity anomaly is imaged with the same shape as in the reference. This is

probably linked to the depth of the targeted structures. Indeed, the cross-lines 20 m (not shown here), proved to be mainly helpful to image 3D structure in the first meters below the surface (surface deposits).

4 Conclusions

In this paper, we propose an innovative methodology to collect efficiently 3D electrical resistivity surveys. We combined the standard 2D parallel acquisition with cross-line measurement, using the roll-along technique in the perpendicular direction. In contrast to existing procedures, we include more than one direction in cross-line measurements using dipole-dipole configurations similar to what can be done in cross-borehole surveys.

We applied this methodology on a synthetic case. It proves that such a data set is informative to image the 3D resistivity structure of the subsurface. Especially, it is important to collect 3D measurements with a depth of investigation coherent with the expected structure of the subsurface. However, the collection of cross-line measurements must not be in detriment of a sufficiently small spacing between parallel lines.

Those results were validated by a field case study. We acquired on the field the proposed 3D in-line/cross-line surveys to image limestone formations subject to karstic features within the context of a wind turbine project. Our methodology enabled to successfully image the presence of a central unaltered limestone ridge surrounded by much less competent rock affected by karstic phenomena. The comparison with standard parallel 2D surveys clearly highlighted the added value of the cross-lines measurements to detect those structures. It provides crucial insight in subsurface geometry for the positioning of a future wind turbine foundation, to the best of our knowledge of the site. The developed method and its modeling results can provide a useful tool in pre-construction 3D subsurface characterization to gain in depth technical insight.

The acquisition of the 3D survey induces additional field and processing work, with an extra cost of about 50%, but those are compensated by the more accurate information brought by the survey. Future work should concentrate on the optimization of cross-line measurements in order to reduce the acquisition time of such surveys. Effort should be made to create an integrated site investigation framework for the characterization of geo-hazardous environments affected by karst features in the light of pre-construction risk analysis, combining geotechnical and geophysical survey methods such as cone penetration testing in combination with 3D ERT and seismic surveying.

Acknowledgments. We would like to thank the geophysical exploration company G-tec S.A. for giving us the opportunity to work on the field site, and for their help on the field for collecting the data. We would like to thank Windvision, for providing us the permission to work on their site and their interest in this work. We thank the Belgian American Educational Foundation and Wallonia-Brussels International for their financial support of T. Hermans.

References

1. LaBrecque, D.J., Ramirez, A., Daily, W., Binley, A., Schima, S.A.: ERT monitoring of environmental remediation processes. *Meas. Sci. Technol.* **7**, 375–383 (1996)
2. Dey, A., Morrison, H.F.: Resistivity modeling for arbitrarily shaped two-dimensional structures. *Geophys. Prospect.* **27**, 106–136 (1979)
3. Nimmer, R.E., Osiensky, J.L., Binley, A.M., Williams, B.C.: Three-dimensional effects causing artifacts in two-dimensional, cross-borehole, electrical imaging. *J. Hydrol.* **359**, 59–70 (2008). doi:[10.1016/j.jhydrol.2008.06.022](https://doi.org/10.1016/j.jhydrol.2008.06.022)
4. Dahlin, T., Bernstone, C., Loke, M.H.: A 3-D resistivity investigation of a contaminated site at Lernacken, Sweden. *Geophysics* **67**, 1692–1700 (2002). doi:[10.1190/1.1527070](https://doi.org/10.1190/1.1527070)
5. Cho, I.-K., Yeom, J.-Y.: Crossline resistivity tomography for the delineation of anomalous seepage pathways in an embankment dam. *Geophysics* **72**, G31–G38 (2007). doi:[10.1190/1.2435200](https://doi.org/10.1190/1.2435200)
6. Marion, J.-M., Barchy, L.: Carte géologique de Wallonie, Chimay-Couvin 57/7-8. Carte Géologique de Wallonie (1999a)
7. Marion, J.-M., Barchy, L.: Carte géologique de Wallonie, Chimay-Couvin 57/7-8. Notice Explicative. Carte Géologique de Wallonie (1999b)
8. Samyn, K., Mathieu, F., Bitri, A., Nachbaur, A., Closset, L.: Integrated geophysical approach in assessing karst presence and sinkhole susceptibility along flood-protection dykes of the Loire River, Orléans, France. *Eng. Geol.* **183**, 170–184 (2014). doi:[10.1016/j.enggeo.2014.10.013](https://doi.org/10.1016/j.enggeo.2014.10.013)
9. Sabbe, A.: Le risque karstique dans les constructions d'habitations-propositions de mitigation. In: *Karst et Aménagements Du Territoire*. Presented at the Karst et Aménagements du territoire (2005)
10. Alija, S., Torrijo, F.J., Quinta-Ferreira, M.: Geological engineering problems associated with tunnel construction in karst rock masses: the case of Gavarres tunnel (Spain). *Eng. Geol.* **157**, 103–111 (2013). doi:[10.1016/j.enggeo.2013.02.010](https://doi.org/10.1016/j.enggeo.2013.02.010)
11. Loke, M.H., Acworth, I., Dahlin, T.: A comparison of smooth and blocky inversion methods in 2D electrical imaging surveys. *Explor. Geophys.* **34**, 182–187 (2003). doi:[10.1071/EG03182](https://doi.org/10.1071/EG03182)